

## Bolometer measurements and transport simulations of the density limit on the W7-AS stellarator

L. Giannone, E. Bellido, R. Brakel, R. Burhenn, R. Dux, A. Elsner, S. Fiedler, T. Geist,  
P. Grigull, H. Hacker, H. Hartfuss, A. Herrmann, J.P.T. Koponen, F. Penningsfeld,  
G. Pereverzev, U. Stroth, F. Wagner, NBI Team and the W7-AS Team.

Max-Planck-Institut für Plasmaphysik, EURATOM Association, D-85748 Garching, Germany

### 1. Introduction

A theoretical basis for understanding the density limit is of importance for a fusion reactor as high edge densities will be needed for power handling. Basic aspects of the density limit can be described by a simple two point power balance of the scrape off layer (SOL) [1,2]. This model assumes pressure constancy and classical parallel electron thermal conductivity along field lines and stable thermal equilibrium in front of divertor/limiter plates with detachment at the density limit when power balance in front of the limiter can no longer be supported. The radiation term in the power balance equation assumes radiation from carbon (coronal equilibrium) in the SOL. The electron density and temperature measurements at the limiter and last closed flux surface, together with the bulk density, temperature and radiation profiles are the experimental quantities of interest. Using the 4 equations of the two point model for a limiter machine [2], the edge density,  $n_s$ , as a function of electron temperature at the limiter,  $T_{lim}$ , for a given temperature fall off length,  $\Delta_T$ , and net power flux at the last closed flux surface,  $q_{\perp}$ , can be predicted.

In W7-AS a discharge with rising line integrated electron density reaching a density limit is shown in Fig.1. The sudden degradation in confinement leading to a decrease in the diamagnetic energy indicates the density limit. In contrast to tokamaks [3,4], current free stellarators at the density limit do not suffer from MHD disruptions and can even recover to a steady state.

This paper is a first attempt to apply the simple two point model to density limit experiments in the W7-AS stellarator. The time dependent ASTRA code [5] was coupled to the impurity transport code STRAHL [6] to facilitate modelling of the radiation profile measured by bolometry. The addition of the simple two point model to ASTRA allowed time dependent simulations of the measured density and temperature at the limiter.

### 2. Experiments and comparison with the two point model

A magnetic field scan from 0.6 T to 2.5 T in NBI discharges with 1100 kW absorbed power, a rotational transform,  $\iota$ , of 0.43 and an upward density ramp was performed. At the lowest and highest magnetic field the total radiated power is 35% and 70% of the input power respectively. This procedure was repeated in discharges at 1.25 T and 2.5 T for absorbed powers from 380 kW to 1440 kW with  $\iota = 0.34$ . The edge densities were taken to be 0.25 of the line averaged density and these values are in good agreement with those from the lithium

beam and Thomson scattering diagnostics.

The two point model was adapted for W7-AS and compared with data from these power and magnetic field scans. From the difference between the input power and bolometer measurements of the bulk radiated power,  $q_{\perp}$  can be calculated. The experimental observation of rising radiated power and decreasing  $q_{\perp}$  with rising line integrated density means that a critical edge density will be reached where  $q_{\perp}$  is no longer sufficient to maintain power balance. Shown in Fig.2, for a typical case in W7-AS with  $\Delta_T = 1, 2$  or 3 cm, and a connection length to the limiter plate,  $L_c$ , of 18 m, this maximum  $n_S$  at the density limit is plotted. It can be seen from the magnetic field scan that for low magnetic field a  $\Delta_T > 3$  cm is suggested, well above the maximum indicated by scaling studies.

### 3. Scaling

The scaling of  $n_S$  with  $q_{\perp}$  and  $B_0$  found by regression analysis, as shown in Fig. 3, is  $n_S = 0.52 q_{\perp}^{0.5 \pm 0.2} B_0^{0.8 \pm 0.15}$ . This scaling can be compared to that found in density limit studies for JET limiter discharges with coefficients of 0.66 and 0.33 respectively [2]. The JET scaling is close to that expected when Bohm diffusion is assumed for the scaling of  $\Delta_T$ . In the case of the  $B_0$  scan on W7-AS, the plasma is pushed up against the inboard limiters. To first order it is expected that  $L_c$  remains constant as a function of  $B_0$  so that the geometrical heat flux enhancement factor,  $L_c/\Delta_T$ , on the left hand side of the power balance equation is not varying significantly with  $B_0$ . In the case of the power scan series, obtaining probe measurements at the limiter involves the compromise of using the up/down limiters which are tangential to the last closed flux surface. This introduces the complication that  $L_c$  will be a function of  $\Delta_T$  and  $B_0$ . It may be possible to explain the stronger  $n_S$  scaling with  $B_0$  in W7-AS and the apparently large  $\Delta_T$  inferred in the above section by a detailed consideration of the  $L_c$  dependence of  $\Delta_T$  and  $B_0$ .

Compared to ASDEX and ASDEX Upgrade density limit discharges, the Greenwald limit for W7-AS in the large aspect ratio, low beta circular approximation appears to be at least a factor of 2 greater but because of the discussed configuration considerations in W7-AS, the usual scaling may not be valid.

### 4. Transport simulations

The values of  $n_S$  from the lithium beam and the measured radiation profiles to calculate  $q_{\perp}$  were taken as inputs while a constant  $\Delta_T = 1.5$  cm was assumed. The time evolution of temperature and density measured by Langmuir probes in front of the limiter in the density limit discharge at 2.5 T with 380 kW NBI input power can then be predicted and are compared to the Langmuir probe measurements in Fig.4. The general features of a rising electron density and falling electron temperature at the limiter can be reproduced and the collapse of the discharge begins as the temperature at the limiter reaches 10 to 20 eV in both the simulation and experiment. From the lithium beam measurements it is clear that the edge density rises continuously to the point of the collapse in diamagnetic energy and that a sudden increase in the density fall off length occurs in the collapsing phase of the discharge, while Langmuir probe measurements indicate that the edge density remains constant for a further 50 ms in the collapsing phase of the discharge.

Impurity puffing experiments were conducted to increase the radiated power and reduce

the power flux so that a density limit could be reached in a similar discharge at a lower edge density. In NBI discharges with 380 kW of deposited power at 2.5 T, nitrogen gas was introduced. For this impurity, the radiation rate coefficient is strongest at 10 eV and with a second maximum at 100 eV and total radiation is proportional to the impurity ion and electron density. The impurity ion density profile for a given impurity flux rate assuming a diffusion coefficient of 0.2 m<sup>2</sup>/s and an inward pinch of 5r/a m/s as calculated by STRAHL and the electron density profile measured by Thomson scattering or an 8 channel microwave interferometer allows the radiated power to be calculated. In discharges without nitrogen gas puffing, carbon was assumed to be the dominant impurity. Impurity concentrations of 15% and 5% in discharges with and without impurity puffing were necessary to reproduce the total radiated power preceding the collapse of the discharge at the density limit. In discharges with impurity puffing, toroidally separated bolometer cameras indicate that impurity gas injection produces significantly more radiation in the vicinity of the gas inlet valve and MARFE formation was observed. In discharges where the impurity gas puffing was systematically increased the density limit decreased.

## 5. Conclusions

Density limit discharges in power and magnetic field scans in W7-AS have been compared to the predictions of the two point model. At low magnetic field, a  $\Delta_T$  greater than 3 cm is inferred, well above the maximum indicated by sealing studies. A stronger  $n_S$  scaling with  $B_0$  compared to JET is found. It is speculated that these two observations can be accounted for by variations in  $L_c$  as a function of  $\Delta_T$  and  $B_0$ . Transport simulations of the time evolution of the density and temperature in front of the limiter according to the two point model were found to reproduce the experimental features of a rising density and falling temperature preceding the density limit. This implies that the limit to the maximum allowable edge density for a given  $q_{\perp}$  necessary to satisfy power balance, with the collapse occurring for a temperature at the limiter of 10-20 eV, is the relevant mechanism determining the density limit in W7-AS.

Helpful discussions with K.Borrass and R.Schneider are gratefully acknowledged.

## 6. References

- [1] D.E.Post and K.Lackner, „Physics of Plasma Wall interactions“, Plenum Press, New York, 1986.
- [2] K.Borrass, D.J.Campbell, S.Clement and G.C.Vlases, Nuclear Fusion, 63, 33, 1993
- [3] A. Stubler et al., Nuclear Fusion, 1557, 32, 1992
- [4] W.Suttrop et al., Nuclear Fusion, 119, 37, 1997
- [5] G.Pereverzev, P. Yushmanov, A. Dnestrovskii, A. Polvoi, K. Tarasjan and L. Zakharov, „An Automatic System for Transport Analysis in a tokamak“, IPP Report 5/42, 1991.
- [6] K.Behringer, „Description of the Impurity Transport Code STRAHL“, JET Report, JET-R(87)08, 1987.

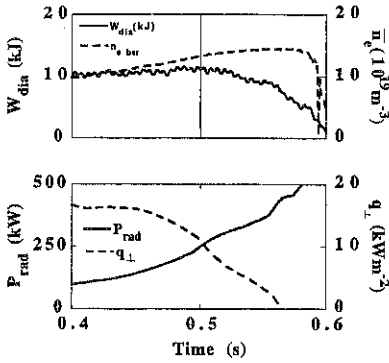


Fig 1. Diamagnetic energy, line integrated density, radiated power and net heat flux at the plasma edge for a density limit shot. Discharge reaches density limit at 0.5 s with a sudden fall in the diamagnetic energy.

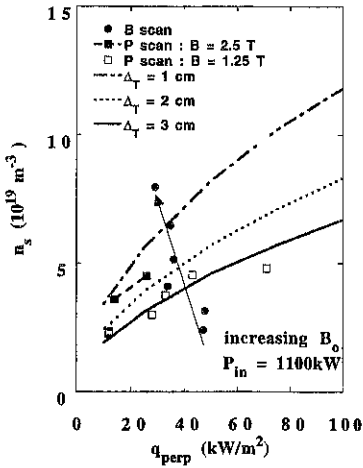


Fig 2. Predicted maximum edge density as a function of heat flux value at the last closed flux surface for various values of the temperature fall off length,  $\Delta_T$ , and  $L_c = 18$  m with experimental point from the power and B scan.

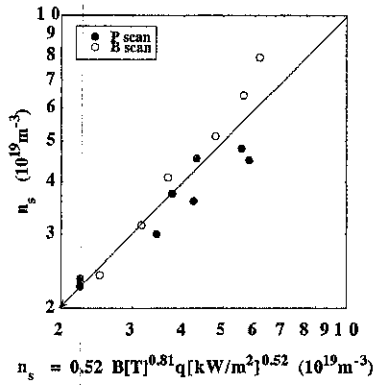


Fig 3. Edge density at the density limit scaling with respect to the magnetic field and perpendicular heat flux with errors of  $\pm 0.15$  and  $\pm 0.2$  respectively in the power law coefficients.

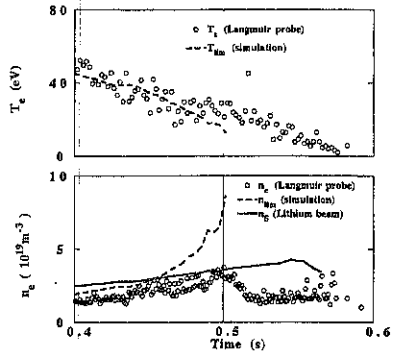


Fig 4. Time evolution of limiter temperature and density compared to the calculated values from the two point model. At 10-20eV, the maximum allowable edge density,  $n_s$  is reached and the discharge collapses.